

WEAR SYNERGY OF COPPER-IRON MIXTURES PROCESSED BY POWDER METALLURGY

W. Aperador^{1,✉}, J. Bautista-Ruiz² and J. Caicedo³

¹Department of Engineering, Universidad ECCI, Bogotá, Colombia, 11101.

²Faculty of Engineering, Universidad Francisco de Paula Santander, San José de Cúcuta, Colombia, 540005.

³Department of Physics, Universidad del Valle, Cali, Colombia, 760034.

✉Corresponding Author: g.ing.materiales@gmail.com

ABSTRACT

Through the powder metallurgy process, copper and iron powders were mixed in the proportions Cu between 15% to 75% and iron from 25% to 85% that made up the binary material systems. The X-ray diffraction technique was used to determine the crystalline structure. Material systems were topographically characterized with optical microscopy. Tribology tests were established using a pin on the disk tribometer. It was determined that the stability of the mixture has different behaviors depending on the evaluated system because the wear system caused, indicating that the phenomenon can be additive. The mixed material is characterized by high friction coefficient and high wear due to the samples' specific properties by increasing the amount of iron in the mixture. The systems analyzed indicate that mechanical degradation was mainly reduced. Dimensional variation of the study specimens was evidenced due to the influence of copper in the system. Only the austenitic structure of the steel was observed, which indicates a complete diffusion of the copper.

Keywords: Powder Metallurgy, Copper, Iron, Corrosion, Wear

RASĀYAN *J. Chem.*, Special Issue, 2021

INTRODUCTION

Powder metallurgy is a process developed by thermal treatment of powders under heat and pressure, obtaining metallic or ceramic compaction at controlled temperatures and below the mixture's melting temperature.^{1,2}

The powder metallurgical process is used to increase the pieces' mechanical resistance due to the high homogeneity and control of the size of the grains. These factors are essential for forming strong bonds between the particles and increasing hardness and toughness.³ In powder metallurgy, materials reduced to compressed powders are used inside molds that shape the part.⁴ Later, the molds are sintered at high temperatures. By sintering, it is possible to join metallic alloys that are difficult to be combined (because they are refractory or because they have very different melting temperatures), allowing the production of parts from complex melting, forging, and machining materials.⁵

The use of powder metallurgy has become popular on an industrial scale because it has allowed the development of advanced materials, obtaining metal parts that are difficult to manufacture with excellent tolerances, high quality, and series production. The industrial application of the Fe-Cu binary alloy system covers sintered stainless steels such as different types of filters and ABS rings for automobiles. Also, equipment such as utensils and kitchen accessories in the food industry. In powders' production, various procedures are used to obtain the required characteristics, considering it necessary to mix powders of different sizes and compositions. Mixing time can vary from a few minutes to several days, depending on the material and the desired results.⁶

Iron and copper mixtures increase the matrix resistance, improve wear resistance, provide antifriction qualities, and resist atmospheric corrosion and chemical agents, especially in contact with sulfuric acid.⁷ The hardening of iron due to the dissolution of copper in the crystalline lattice develops greater resistance and hardness. This type of material is consolidated by an atypical cold pressing process and subsequent

sintering.⁸ Some research highlights that the Fe-Cu intermetallic compound has shown the best wear and corrosion properties by varying factors such as temperature, time, pressure, and chemical composition to obtain parts with the appropriate characteristics.⁹

The effect of copper on steel improves mechanical resistance provides good resistance to impact and abrasion. Copper has been used in high-alloy and stainless steel to improve corrosion resistance. Copper has been used in stainless and high-alloy steels to improve corrosion resistance in specific environments, reduce susceptibility to stress corrosion cracking and provide age hardening.¹⁰

This research used iron and copper powders to modify the tribological and electrochemical properties. For this purpose, the addition of copper powders in proportions of 15% - 75% of the alloying element was studied. Research shows that materials with copper additions between 60% and 75% have good tribological and electrochemical characteristics when evaluating friction coefficients and wear rates, respectively.

EXPERIMENTAL

Before the manufacturing process, an analysis of the powders was developed in its conditioning process, including the materials compaction and subsequent sintering. Iron and copper powders of 99.9% purity and particle size of ~ 80 μm were used in the conditioning process. The powders were mixed according to the following compositions Cu15% -Fe85%, Cu30% -Fe70%, Cu45% -Fe55%, Cu60% -Fe40%, Cu75% -Fe25%. The mechanical alloying was made in a hardened steel ball mill with a ball-powder weight ratio of 4:1.

A uniaxial force was applied to utilize a Universal Electromechanical Testing Machine type INSTRON model 4507 with a maximum load cell of 100 kN. The machine is equipped with a conventional resistance oven that allows working at a maximum of 1300 °C. A mold was also used that allowed the controlled compaction of the material at 0.5 mm/s and a load of 7.1×10^3 kgf/cm².

The powder falls by the gravitational force from the filling device into the mold cavity. The mold is provided with a cylindrical sleeve with a lower cover held by three screws. The punch was located inside the jacket and received the load employing a disk in charge of uniformly transporting the force of the Universal Machine to the powder. Therefore, its geometry was specific, and it was adapted to the upper plate of the machine.

The mixed powder material was processed in a uniaxial compression fashion. Subsequently, the compound was sintered, starting with a heating ramp up to 300 °C in 120 minutes. This temperature is required for phase separation in solid polycrystalline Fe-Cu solutions. Then the ramp was raised for 120 minutes until reaching 500 °C, holding it for 120 minutes.

To obtain a dense material and evaluate the possible effect of pores on the wear properties of the alloy, the following experimental methodology was developed: after filling the mold, the powder is compressed in a single normal direction. The base and the walls of the part are stationary. The pressing operation is carried out only by the upper punch when it moves within the fixed die. As the friction of the matrix walls prevents uniform distribution, pressure is applied until the metallic aggregate with the desired density is obtained (the compact material has a higher density in the upper part than in the lower part). Three stages qualitatively describe this process:

(1) for low pressures, the reduction in porosity is due to a mechanism for re-accommodating the particles without undergoing deformation. For specific pressure values, packing stabilizes, and densification is only possible by elastic and plastic deformations of the particles through their contact areas.

(2) stress multiplies with elastoplastic deformation, and

(3) the plastic deformation extends to the entire particle. The material increases resistance to plastic flow due to deformation hardening of the particles and geometric hardening due to the progressive increase in their contact areas. Its compressibility decreases drastically, not only due to hardening phenomena but also due to the effect of air and lubricant trapped in pores. Therefore, the metallic compact is a packing of deformed particles that can move to each other. The essential characteristics of granular material are inter-particle porosity and sliding between said particles through their contacts.

The structural characterization of the mixtures was developed by the X-ray diffraction technique using a Bruker D8 Advance A25 equipment with Co-K α monochromatic radiation of a wavelength of 1.78900 Å, Bragg-Brentano geometry, goniometer in θ/θ configuration in a 2θ range between 10° and 90°, a step of

0.02° and time of 2s, respectively. The different crystalline phases were identified during the characterization by comparing the diffractions with the database (Crystallography Open Database). Additionally, Rietveld refinement was applied.

A pin on disk equipment was used for the wear study, with flat specimens and a 50 m/min rotation speed. The tribological pair consisted of the AISI Cr 52100 steel pin and the samples obtained by powder metallurgy. The tests were carried out at 25 °C (room temperature).

The optical evaluation was carried out at 100 X through an Optical Microscope with LECO 500 Image Analyzer. Surface homogeneity and the transverse plane related to the compaction direction were observed. This technique required metallographic preparation of the specimen until dry polishing with abrasive papers number 2500 and dry cloth with diamond dust. As attack reagents, the following were used: a) 45 cm³ of HCl, 15 cm³ of HNO₃, and 20 cm³ of ethanol.

RESULTS AND DISCUSSION

Figure-1 shows the spectra of the iron-copper alloy obtained according to the compositions Cu15%-Fe85%, Cu30% -Fe70%, Cu45% -Fe55%, Cu60% -Fe40% and Cu75% -Fe25%. The study shows that the phases with the highest intensity correspond to the ternary oxide CuFeO₂ in-plane reflection (110) related to a rhombohedral symmetry, as shown in Fig.-2a.¹¹ The phase formation is due to the transition from Cu²⁺ to Cu¹⁺ during the powder metallurgy process.¹² The parameters for this phase are a = b = c = 5.90 Å, α = β = γ = 29.430 ° and space group R-3m. The same ternary oxide of CuFeO₂, but with less peak intensity, is found in the reflection of planes (112) and (222). The Fe85% Cu15% and Fe25% Cu75% systems show that the alloys are almost single phases. The network parameters correspond to copper with values of a = b = c = 3,615 Å and α = β = γ = 90 °, and for Fe a = b = c = 2,866 Å and α = β = γ = 90 °. For these alloys, reflections are located for Fe in the (100) and (211) planes and Cu in the (111), (200), and (311) planes. The biphasic alloy, corresponding to CuO, has a plane associated with reflection (131).¹³ Reflections and intensity indicate that each processed mixture has formed a solid replacement solution. The effect of copper on iron is evidenced by comparing the crystalline structures of the samples Cu15%-Fe85%, Cu30%-Fe70%, Cu60%-Fe40%, and Cu75%-Fe25%. For the systems Cu60%-Fe40% and Cu75%-Fe25%, peaks with greater intensity are observed due to the greater solubility of copper.¹⁴

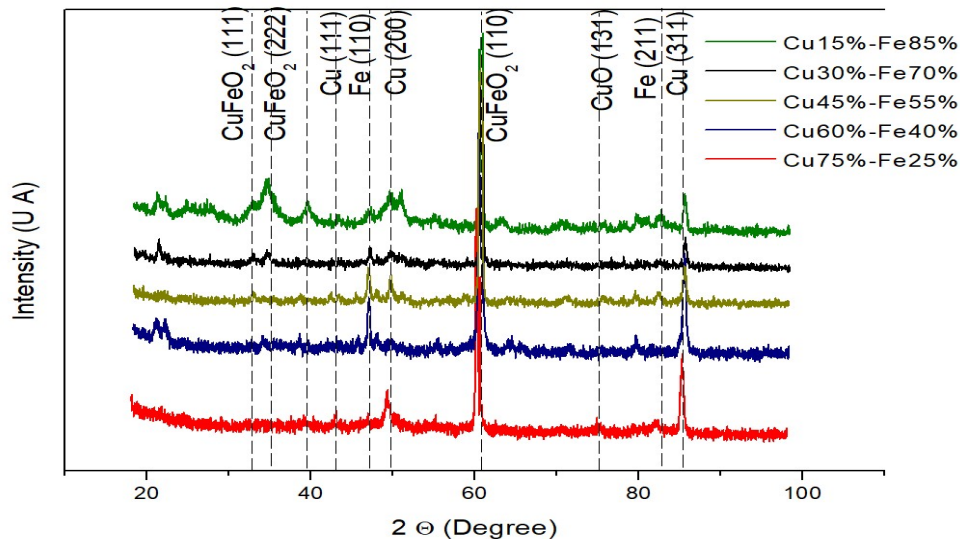


Fig.-1: X-ray Diffraction Spectra Corresponding to the Systems Cu15%-Fe85%, Cu30%-Fe70%, Cu45%-Fe55%, Cu60%-Fe40% and Cu75%-Fe25%.

Figure-2 is the result of the analysis deterioration by corrosion. The potentiodynamic curves show that the mixtures generalized type corrosion due to the passive layers. This passive layer acts synergistically and inhibits the potentially damaging pitting corrosion process.¹⁵⁻¹⁷ The materials obtained by powder metallurgy and evaluated for corrosion show lower corrosion rates. The Cu75%-Fe25% system decreased the corrosion rate values by two orders of magnitude. For the dual evaluation, the corrosion current density

was 1.39×10^{-7} A/cm² and 1.74×10^{-5} A/cm² in the study of corrosion. Reducing the corrosion current is directly related to the corrosion rate decrease by increasing alloying iron percentage.¹⁸⁻¹⁹ From the results found, it is possible to infer that the best systems evaluated by corrosive contain the highest percentage of copper content. This result is due to physical-chemical conditions because copper metal oxides are stable to oxidation reactions with ions present in saline solution. Therefore, the corrosion rate values are related to the studied materials' chemical and mechanical reactions.

Figure-3a, 3b, 3c, 3d and 3e show the results of atomic force microscopy and correspond to the surfaces of the study materials after the mixing and sintering processes. The surfaces were polished with silicon carbide (SiC) abrasive papers with granulometry 220, 340, 400, 600, 1200, 1500, and 2000. The final finish was given with a polishing machine and 0.05 μm alumina.

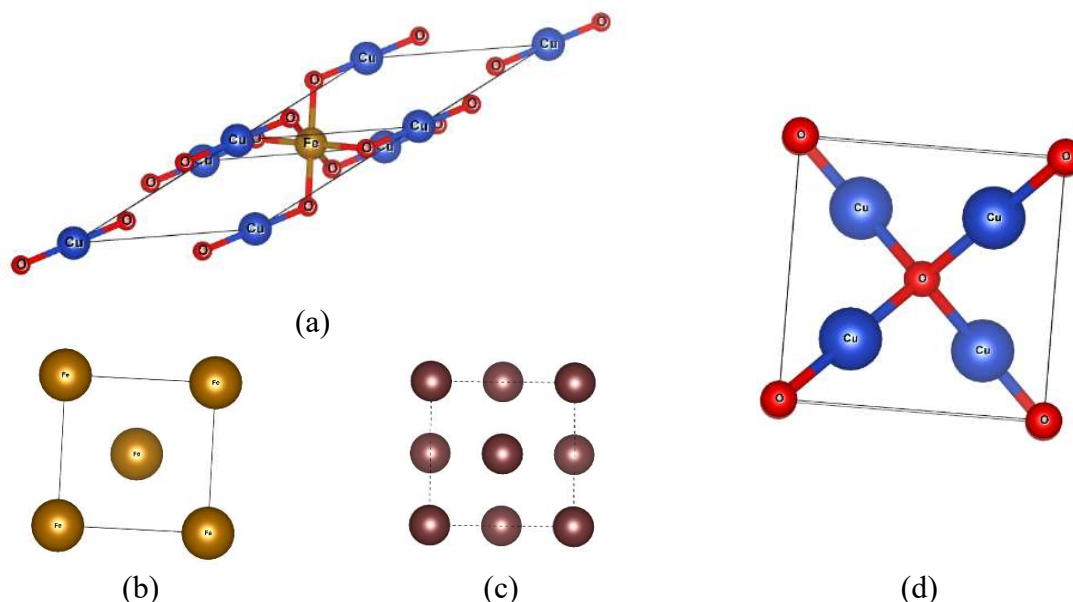


Fig.-2: Structural Configurations of the Cu-Fe Compounds obtained via Powder Metallurgy.

Figure-3 shows the variations in friction forces as a function of distance. The measurements were taken in the evaluation range of the COF. The friction force determines the natural contact area and its relationship with the materials' surface morphology due to the granulometry that makes it up.²⁰ Smaller grain sizes were found for composite systems with larger copper ones. This trend was evidenced in the intensity of the peaks of the diffraction patterns. In the samples Cu15%-Fe85% and Cu30%-Fe70%, peaks with greater intensity and little amorphous phase were identified. For the systems Cu45% -Fe55% and Cu60% -Fe40%, friction force values lower than 1 N was determined and considered solid lubricant. The variations found at values after 20 m in the Cu60%-Fe40% system are related to the surface roughnesses obstructing the indenter's displacement.²¹ A greater smooth surface area is shared as the indenter slides, explaining the different friction force alterations in each system studied. For the samples Cu75% -Fe25%, it is observed that the friction force is independent of the load applied in the segment from 0 to 50 m. The friction force values are the lowest of all the systems evaluated (Fig.-4). Due to this type of behavior, the surface is considered smooth with low friction.²² Analysis after 60 m shows that the friction force is dependent on the contact area. A greater friction force is required, and it is the material's response due to the roughness due to the lower atomic radius value of copper and its high concentrations added to the matrix, shrinkage of the samples due to re-stacking phenomena expected. The wear resistance of steel would practically not improve. For the high content of copper added to the steel matrix, there is a substantial increase in wear resistance correlated with the decrease in the value of the friction coefficient. In addition, it was observed that the wear resistance reaches the highest values for the alloy Cu60% -Fe40%. This behavior is due to the more significant hardening produced by copper in this proportion. In conclusion, the Cu60% -Fe40% alloy is more effective than mechanical.

Sintering at 1150°C, it was observed that when 15% copper was introduced into the steel matrix, the alloying agent was completely diffused. Thus, in stainless steels alloyed with 30%, 45%, 60%, and 75% copper, only the austenitic structure of the steel is evidenced, which indicates a complete diffusion of the copper. It was also observed that the austenitic phase increases proportionally to the content of copper in the alloy.

Regarding the dimensional variation, swelling of the steel matrix was observed when adding copper in the study concentrations when sintering at 1150 °C, as shown by Yang et al. in their research.²³

Dimensional variation of the study specimens was evidenced due to the influence of copper in the system. However, due to the lower atomic radius value of copper and its high concentrations added to the matrix, shrinkage of the samples due to re-stacking phenomena is expected. This behavior would be observed for copper aggregations lower than 15%.

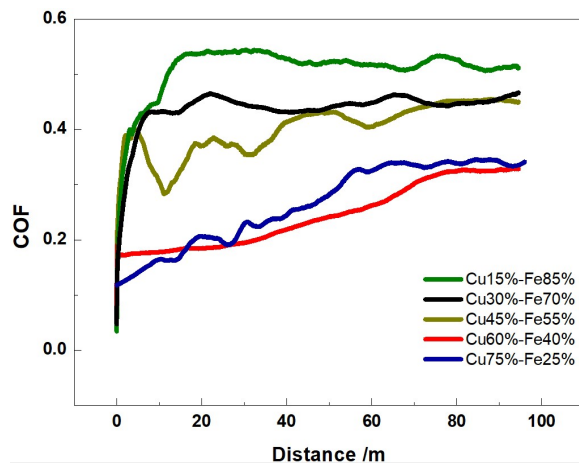


Fig.-3: Graphs of the Friction Coefficient corresponding to the Systems Cu15%-Fe85%, Cu30%-Fe70%, Cu45%-Fe55%, Cu60%-Fe40% and Cu75%-Fe25%.

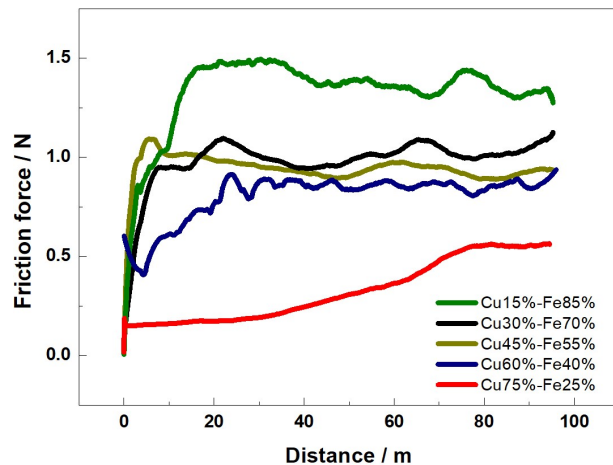


Fig.-4: Graphs of Friction Forces corresponding to the Systems Cu15%-Fe85%, Cu30%-Fe70%, Cu45%-Fe55%, Cu60%-Fe40% and Cu75%-Fe25%.

In the micrographs of Fig.-5, heterogeneous surfaces are observed. The roughness values were determined for each system studied, resulting in at 857 pm for the 15%Cu-85%Fe system, 848 pm for the 30%Cu-70%Fe system, 399 pm 45%Cu-55%Fe system, 175 pm for the 60%Cu-40%Fe system, and 129 pm for the 75%Cu-25%Fe system. In the two systems with greater roughness, pores are observed. In the other systems, smooth surfaces can be related to the powder metallurgical process, where the pressing process improves the adherence between the copper particles and facilitates the formation of bonds. Subsequently, the sintering process homogenizes and fuses the powders. The metallographic study (Fig.-5) shows similar microstructures for the copper alloy. Alloys with percentages greater than 15% copper showed an epsilon phase along the austenite grain boundaries and are believed to be proeutectoid in origin. In the development of this study, the austenite phase was found in the iron-copper system.

Figure-6 shows the micrographs of the corrosion-wear process. The response of the samples to NaCl is evidenced, showing continuous wear caused by the pin and the formation of a passive layer without deterioration. It is appreciated that, in travel, the pin did not wear the passive film significantly due to the conditions associated with the adhesion of the film. This behavior is observed in all the analyzed systems. In the systems' tracks, areas with brown streaks attributed to material contributed by the pin during the test were observed due to the contact and detachment of material between the two bodies.²⁴

Contact with the sphere generated minor wear on materials with high copper content. In these systems, no localized corrosion attack was observed due to the low activity in the time-current series compared to the system's oxide film without wear, where this type of corrosion was created. According to the results, the dual corrosion-wear effect is beneficial due to the activation-passivation process that decreased the corrosion wear activity. The Cu75%-Fe25% system showed the best performance. The results are following that reported by Lazurenco et al.²⁵

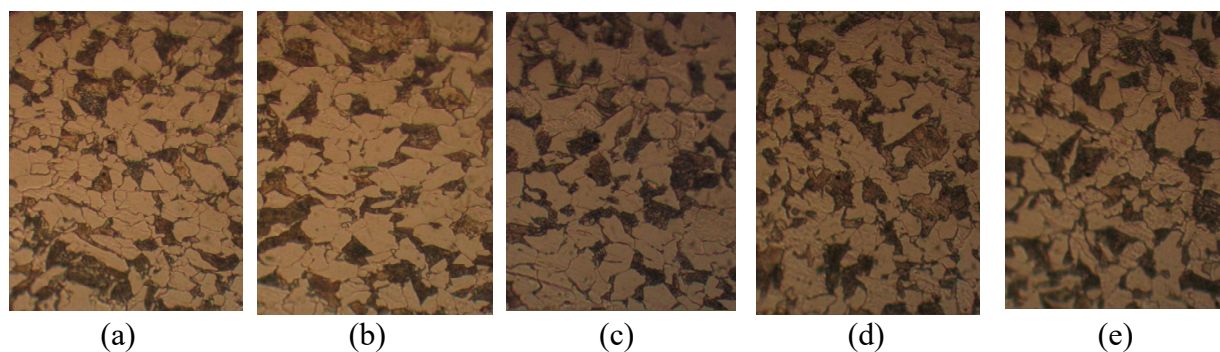


Fig.-5: Optical Microscopy Micrographs (a) Cu15%-Fe85%, (b) Cu30%-Fe70%, (c) Cu45%-Fe55%, (d) Cu60%-Fe40% and (e) Cu75%-Fe25%.

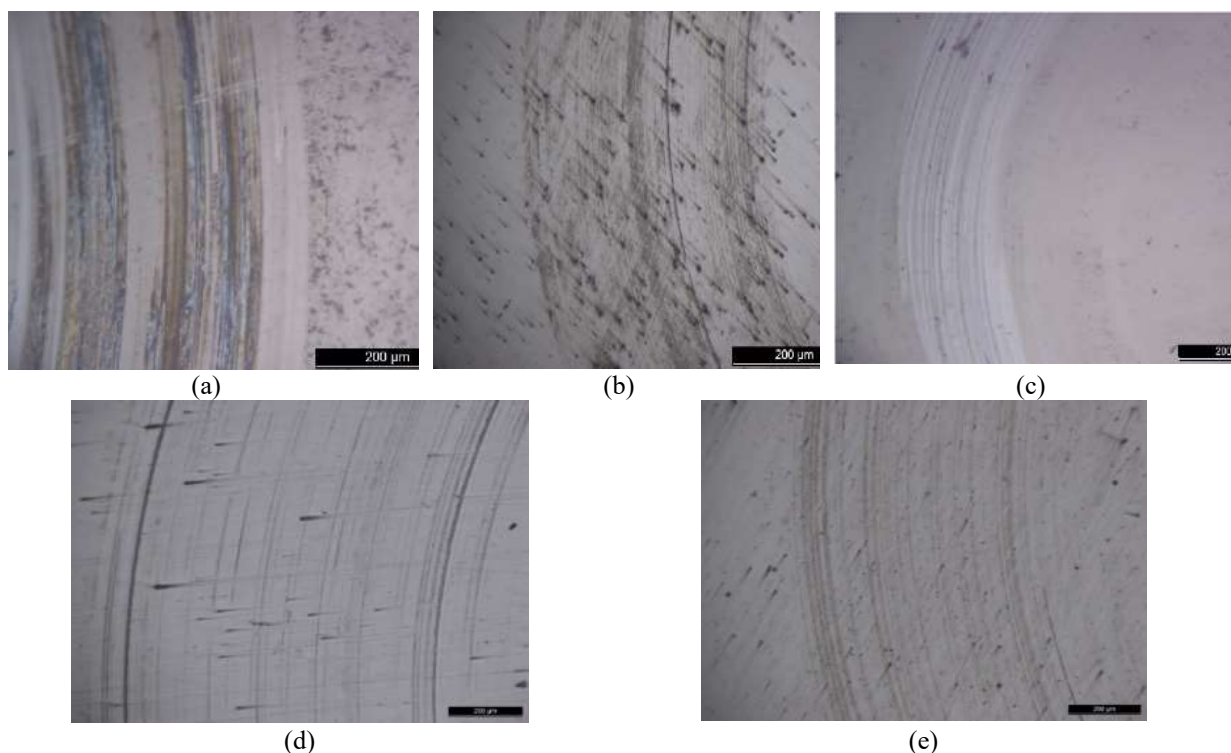


Fig.-6: Micrographs of the Dual Corrosion-wear process (a) Cu15%-Fe85%, (b) Cu30%-Fe70%, (c) Cu45%-Fe55%, (d) Cu60%-Fe40% and (e) Cu75%-Fe25%.

CONCLUSION

Interaction between the surfaces of the sphere used in wear and the specimens of the material mixed between iron and copper is characterized by high coefficients of friction and high wear due to the samples' specific properties by increasing the amount of iron in the mixture.

The interaction between the corrosive fluid and the two materials that make up the tribological pair consisted of generating an interface between the surfaces in contact and relative movement. The intermediate material is the liquid that is responsible for the degradation in the case of static, consequently, the wear. Therefore, all the systems analyzed indicate that mechanical degradation was mainly reduced. Systems with a lower coefficient of friction values perform additional functions due to the decrease in wear and corrosion current values that depend on the percentages of copper added to the mixture. In the case of tribocorrosion, the permanent contact of the parts and the elimination of impurities make the system improve the anticorrosive response.

REFERENCES

1. D. Chaira, *Science and Materials Engineering*, **2**, 588(2021), <https://doi.org/10.1016/B978-0-12-803581-8.11703-5>

2. H.A. Macías, L. Yate, E. Coy, *Applied Surface Science*, **558**, 149887(2021), <https://doi.org/10.1016/j.apsusc.2021.149877>
3. S. Jyothi, Y.V. Subba Rao and P.S. Samuel Ratnakumar, *Rasayan Journal of Chemistry*, **12(2)**, 537(2019), <https://doi.org/10.31788/RJC.2019.1225000>
4. J. Duan, M. Zang, P. Chen, Z. Li, L. Pang, P. Xiao and Y. Li, *Ceramics International*, **47(14)**, 19271(2021), <https://doi.org/10.1016/j.ceramint.2021.02.187>
5. R. Thilagavathi, A. Prithiba and R. Rajalakshmi, *Rasayan Journal of Chemistry*, **12(2)**, 431(2019), <https://doi.org/10.31788/RJC.2019.1225133>
6. A. González-Hernández, A. B Morales-Cepeda, M. Flores M, J.C Caicedo, *Coatings*, **11(7)**, 797(2021), <https://doi.org/10.3390/coatings11070797>
7. W. Hung-Kai, W. Zih-Huei and W. Ming-Chi, *Computers & Industrial Engineering*, **148**, 106635(2020), <https://doi.org/10.1016/j.cie.2020.106635>
8. J. Vairamuthu, B. Stalin, G.D. Sivakumar, B. Mohamed Fazil, R. Balaji and V.A. Natarajan, *Materials Today*, **45(2)**, 1970(2020), <https://doi.org/10.1016/j.matpr.2020.09.262>
9. E. Xu, J. Huang, Y. Li, Z. Zhu, M. Cheng, D. Li, H. Zhong, J. Liu and Y. Jiang, *Powder Technology*, **344**, 551(2019), <https://doi.org/10.1016/j.powtec.2018.12.059>
10. J. Bautista-Ruiz, W. Aperador and J.J. Olaya, *Rasayan Journal of Chemistry*, **11(2)**, 597(2018), <https://doi.org/10.31788/RJC.2018.1122075>
11. Mussatto, R. Groarke, A. A-Hameed, I.U.I. Ahad, R.K. Vijayaraghavan, A. O'Neill, P. McNally, Y. Delaure and D. Brabazon, *Materials & Design*, **182**, 108046(2019), <https://doi.org/10.1016/j.matdes.2019.108046>
12. A. H. Omran-Alkayatt, S. M. Thahab, and I. A. Zgair, *Optik*, **127(8)**, 3745(2016), <https://doi.org/10.1016/j.ijleo.2015.12.144>
13. B. B. Vara Prasad, K.V. Ramesh and A. Srinivas, *Solid State Sciences*, **107**, 106325(2020), <https://doi.org/10.1016/j.solidstatesciences.2020.106325>
14. Y. Li, B. Yang, P. Zhang, Y. Nie, X. Yuan, Q. Lei and Y. Li, *Materials Today Communications*, **27**, 102266(2021), <https://doi.org/10.1016/j.mtcomm.2021.102266>
15. M.R. Akbarpour, H. Mousa Mirabad, M. Khalili Azar, K. Kakaei and H.S. Kim, *Materials Science and Engineering: A*, **786**, 139395(2020), <https://doi.org/10.1016/j.msea.2020.139395>
16. X. Ma, C. Luan, S. Fan, J. Deng, L. Zhang and L. Cheng, *Tribology International*, **154**, 106686 (2021), <https://doi.org/10.1016/j.triboint.2020.106686>
17. Y. Bian, J. Ni, C. Wang, J. Zhen, H. Hao, X. Kong, H. Chen, J. Li, X. Li, Z. Jia, W. Luo and Z. Chen, *Materials Characterization*, **172**, 110847(2021), <https://doi.org/10.1016/j.matchar.2020.110847>
18. N. Ravikumar, T.R. Tamilarasan and R. Rajendran, *Carbon Trends*, **3**, 100031(2021), <https://doi.org/10.1016/j.cartre.2021.100031>
19. E.P. Shalunov and Y.O. Vladimirova, *Materials Today*, **38(4)**, 1784(2021), <https://doi.org/10.1016/j.matpr.2020.08.266>
20. H. Zhou, P. Yao, Y. Xiao, K. Fan, Z. Zhang, T. Gong, L. Zhao, M. Deng, C. Liu and P. Ling, *Tribology International*, **132**, 199(2019), <https://doi.org/10.1016/j.triboint.2018.11.027>
21. M.R. Akbarpour, H. Mousa Mirabad, M. Khalili Azar, K. Kakaei and H.S. Kim, *Materials Science and Engineering: A*, **786**, 139395(2020), <https://doi.org/10.1016/j.msea.2020.139395>
22. W. Yang, H. Zhao, K. Wang and C. Zheng, *Proceedings of the Combustion Institute*, **35**, 2811(2015), <https://doi.org/10.1016/j.proci.2014.07.010>
23. E. Kocaman, B. Kılınc, M. Durmaz, Ş. Şen and U. Şen, *Engineering Science and Technology, an International Journal*, **24(2)**, 533(2021), <https://doi.org/10.1016/j.jestch.2020.08.003>
24. P. Yang, H. Fu, R. Absi, R. Bennacer, J. Lin and X. Guo, *Materials Characterization*, **168**, 110577(2020), <https://doi.org/10.1016/j.matchar.2020.110577>
25. D.V. Lazurenko, G.I. Alferova, M.G. Golkovsky, K.I. Emurlaev, Y. Emurlaeva, I.A. Bataev, T.S. Ogneva, A.A. Ruktuev, N.V. Stepanova and A.A. Bataev, *Surface & Coatings Technology*, **395**, 125927(2020), <https://doi.org/10.1016/j.surfcoat.2020.125927>

[RJC-6678/2021]